Epstein-Barr Virus Encodes Three Bona Fide Ubiquitin-Specific Proteases

JOURNAL OF VIROLOGY, Nov. 2008, p. 10477–10486 Vol. 82, No. 21
0022-538X/08/$08.00+0 doi:10.1128/JVI.01113-08

Epstein-Barr Virus Encodes Three Bona Fide Ubiquitin-Specific Proteases▽‡

Ramakrishna Sompallae,[1]† Stefano Gastaldello,[1,2]† Sebastian Hildebrand,[1] Nikolay Zinin,[1] Gerco Hassink,[1] Kristina Lindsten,[1] Juergen Haas,[3] Bengt Persson,[1,4] and Maria G. Masucci[1]*

Department of Cell and Molecular Biology, Karolinska Institutet, S-171 77 Stockholm, Sweden[1]; Department of Biomedical Sciences, University of Padua, 35121 Padua, Italy[2]; Division of Pathway Medicine, School of Biomedical Sciences, College of Medicine, University of Edinburgh, Edinburgh, United Kingdom, and Max von Pettenkofer-Institute, LMU-München, Munich, Germany[3]; and IFM Bioinformatics, Linköping University, S-581 83 Linköping, Sweden[4]

Received 27 May 2008/Accepted 8 August 2008

Manipulation of the ubiquitin proteasome system (UPS) is emerging as a common theme in viral pathogenesis. Some viruses have been shown to encode functional homologs of UPS enzymes, suggesting that a systematic identification of these products may provide new insights into virus-host cell interactions. Ubiquitin-specific proteases, collectively known as deubiquitinating enzymes (DUBs), regulate the activity of the UPS by hydrolyzing ubiquitin peptide or isopeptide bonds. The prediction of viral DUBs based on sequence similarity with known enzymes is hampered by the diversity of viral genomes. In this study sequence alignments, pattern searches, and hidden Markov models were developed for the conserved C- and H-boxes of the known DUB families and used to search the open reading frames (ORFs) of Epstein-Barr virus (EBV), a large gammaherpesvirus that has been implicated in the pathogenesis of a broad spectrum of human malignancies of lymphoid and epithelial cell origin. The searches identified a limited number of EBV ORFs that contain putative DUB catalytic domains. DUB activity was confirmed by functional assays and mutation analysis for three high scoring candidates, supporting the usefulness of this bioinformatics approach in predicting distant homologues of cellular enzymes.

The posttranslational modification of proteins by ubiquitin (Ub) and Ub-like molecules (UbLs) and the degradation of polyubiquitinated substrates by the proteasome regulate fundamental cellular processes, including cell growth and differentiation, intracellular signaling, protein trafficking, apoptosis, and the recognition of virus-infected or malignant cells by the host immune response (21, 27, 33, 44, 46). Modulation of the ubiquitin-proteasome system (UPS) is emerging as a central theme in viral pathogenesis, and several examples have been reported of viral proteins that mimic or redirect the activity of the system in order to modify the cellular environment in favor of virus persistence or replication (22, 28, 31, 34, 41, 45). Thus, the identification of viral products that interfere with the UPS may yield new insights on important features of viral pathogenesis and could lead to the development of new means of therapeutic intervention.

Conjugation of Ub or UbLs is achieved through the activity of a cascade of enzymes, including activating enzymes (E1s), conjugating enzymes (E2s), and specific ligases (E3s) that catalyze the covalent linkage of the modifier to Lys residues in the substrate (11). In addition, deconjugating enzymes act as regulators of the system by maintaining the pool of free Ub and UbLs and by determining the rate of turnover of the conjugates (14, 50). In line with this proposed regulatory function, recent evidence points to a critical role of Ub deconjugases (deubiquitinating enzymes [DUBs]) in intracellular signaling, as exemplified by the activation of the transcription factor nuclear factor-κB (NF-κB) by cylindomatosis tumor suppressor, A20, Cezanne, and ubiquitin-specific protease 31 (25, 33) and by the initiation of DNA repair by USP1 (37).

Based on similarity with known family members, the human DUBs have been classified in five subfamilies including: ubiquitin C-terminal hydrolases (UCHs), ubiquitin-specific proteases (USPs), Machado-Joseph disease proteases (MJDs or Josephins), ovarian tumor proteases (otubains, OTUs), and the JAMM (Jab1/MPN/Mov34 metalloenzyme) motif proteases (2, 38). With the exception of JAMMs, the DUBs are cysteine proteases identified by a catalytic triad of Cys, His, and Asp/Asn residues and by the presence of conserved amino acid domains known as Cys- and His-boxes (C- and H-boxes, respectively) that are unique for each family (38). Mutational studies have shown that the Asp/Asn residue is not essential for catalytic activity, although it may contribute to the enzymatic activity by stabilizing the active-site thiolate and imidazolium ion pair (26, 35). The JAMM metalloproteases lack a C-box, while two conserved His residues in the JAMM motif were shown to be essential for activity (49).

Proteins with DUB activity are encoded in the genome of human adenovirus, herpesvirus, coronavirus, and bunyavirus (5, 6, 18, 29, 42). Furthermore, DUB activity was recently demonstrated in proteins encoded by some pathogenic bacteria that lack an intrinsic UPS (40, 52), suggesting that these enzymes play specific roles in the regulation of both viral and bacterial infection. Although these findings make the systematic identification of microbial DUBs a worthy endeavor, the task is complicated by the wide sequence variation of the known enzymes. Moreover, viral and bacterial proteins are often considerably different in sequence and domain organization compared to their mammalian counterparts, which fur-

* Corresponding author. Mailing address: Karolinska Institutet, Box 285, 171 77, Stockholm, Sweden. Phone: 46 8 52486755. Fax: 46 8 337412. E-mail: maria.masucci@ki.se.

† R.S. and S.G. contributed equally to this study.

‡ Supplemental material for this article may be found at http://jvi.asm.org/.

▽ Published ahead of print on 20 August 2008.

TABLE 1. Data sets of DUBs used in this study

Protein family	Characteristic domain	No. of human DUBs	No. of verified DUBs[a]	No. of orthologs	No. of DUBs in pattern search set[b]	No. of DUBs in HMM training set[d]	
						C-box	H-box
USP	Peptidase 19	45	37		45	36	42
UCHL	Peptidase 12	4	4	15	19	10	8
OTU	OTU	8	5	9	17	10	11
MJD	Josephin	3	1	9	12	7	7
JAMM[c]	MPN+	8	2	29	34		21

[a] That is, the number of DUBs with experimentally verified enzymatic activity.
[b] Due to the small number of identified sequences in the human UCH, OTU, JAMM, and MJD subfamilies, orthologs from other species were included in the data set.
[c] The JAMM metalloproteases contain only H-box domains, and sequence homologs with catalytic. His residues were considered for deriving the patterns.
[d] Only C- and H-boxes with <90% sequence identity were used for training the HMMs.

ther hampers the identification of distant functional homologues.

We have used a bioinformatics strategy here to identify putative virus-encoded DUBs. To overcome the difficulty posed by sequence variation, we focused on the conserved C- and H-boxes. Family-specific sequence alignments, pattern searches, and hidden Markov models (HMMs) were generated based on the amino acid sequences of known members of the five DUB subfamilies and then used to search a custom-made database of open reading frames (ORFs) from Epstein-Barr virus (EBV), a human gamma herpesvirus that establishes latent infections and is associated with a broad spectrum of malignancies of lymphoid and epithelial cell origin.

MATERIALS AND METHODS

Data sets. The sequences of DUBs were extracted from the UniProt database version 51.2 (4). The DUB data set consisted of both experimentally verified human enzymes and highly conserved sequence homologs (Table 1). For families with fewer than 10 human sequences, homologues from other species were included. The sequence of the B95.8 EBV genome (3) was obtained from NCBI GenBank (Refseq NC_007605). The sequences of 75 annotated EBV ORFs were retrieved from the Swiss-Prot database. In addition, ORF prediction was carried out with the getORF program available in the EMBOSS package (39), with a length cutoff setting between 150 and 5,000 amino acids (aa), which resulted in 106 predicted ORFs. For ORFs annotated in Swiss-Prot, the progressive number assigned to the predicted ORFs was substituted with the corresponding gene symbol.

DUB searches. (i) Sequence alignment. Sequence comparisons between the human DUBs and the EBV ORFs were carried out by using CLUSTAL W (47) and BLAST (1). CLUSTAL W calculates multiple sequence alignments and was therefore used to investigate whether any of the EBV ORFs clusters with the specific DUB subfamilies. BLAST searches were used to identify putative C- and H-boxes. To this end, members of each DUB family were aligned by using CLUSTAL W, and conserved catalytic domains were extracted with the GoCore program (http://www.helsinki.fi/project/ritvos/GoCore/). The C- and H-box domains of each family were defined on the basis of the conserved regions (UCH, C-box 23aa and H-box 24aa; USP, C-box 16aa and H-Box 21aa; OTU, C-box 19aa and H-box 14aa; MJD, C-box 21aa and H-box 14aa; JAMM domain 25aa), and the sequences were then searched against the EBV ORF database. Hits with arbitrarily chosen E-values of ≤10 and containing Cys or His residues were selected for further analysis.

(ii) Pattern search. C- and H-box specific patterns were constructed to search for putative catalytic domains. The C- and H-boxes of each DUB family were aligned with respect to the conserved Cys and His residues, and search patterns were manually derived from the sequence alignments based on the physicochemical properties.

(iii) HMM search. HMMs were constructed by using the HMMER (17) suite of programs. For each DUB subfamily the HMMs were trained with multiple sequence alignments of C- and H-boxes from a nonredundant set of sequences (Table 1, HMM training set). The HMM results were further categorized based on E-values and raw scores. In every search with subfamily-specific HMMs, matches with E-values of <25 were selected and manually screened for the presence of Cys or His residues in the alignment. Candidates containing putative C- or H-boxes were further categorized based on the HMM scores of the domains. The HMM score is a base 2 log of the probability of alignment to the HMM divided by the probability of random alignment. A score of zero represents 50% likelihood that the sequence is a true match to the model. Since the EBV ORF database contains 106 entries, scores greater than 6.7 correspond to a 99% probability to detect true homologs while a score of −6.6 corresponds to 1% probability. Due to the fact that the genomes of viral and other pathogenic organisms undergo higher mutation rates (16), low thresholds of statistical parameters were used to detect catalytic domains of DUBs.

(iv) Conserved Cys and His residue search. Homologous proteins that are conserved between members of at least one subfamily of human herpesviruses (α-HHVs: herpes simplex virus type 1 [HSV-1], HHV1, HSV-2, HHV2, varicella-zoster virus, and HHV3; β-HHVs: human cytomegalovirus, HHV5, HHV6, HHV7; and γ-HHVs: EBV, HHV4, Kaposi sarcoma herpesvirus, and HHV8) were identified by using BLAST with a cutoff E-value of 0.01, corresponding 99% probability to be a true homolog. Homologous proteins were then aligned by using Vector NTI (32), and the multiple alignments of each cluster were scanned for the presence of conserved Cys and His residues. Sequences flanking the conserved residues were searched for putative C- and H-boxes using the HMMs.

Functional validation of candidate DUBs: cloning of EBV ORFs into prokaryotic expression vector. ORFs derived from the B95-8 virus were transferred from the GATEWAY expression vector pDONR207 (48) to the prokaryotic expression vector pDEST-GST (ampicillin resistance), and *E. coli* DH5α was used for transformation.

Ub-GFP construct. Green fluorescent protein (GFP) was amplified by PCR from pEGFP-N1 vector (Clontech, Palo Alto, CA) with the sense primer 5′-GTTTTCAGATCTAAAGGAGAAGAGCTGTTCACCGGCGTGAGCAAGGGCGAGGAGCTGTTCACC-3′ and the antisense primer 5′-GTTCTCGAGCTTGTACAGCTCGTCCATGCCGAGAGTGAT-3′ and cloned in the BglII and XhoI sites of the pACYCDuet-1 vector (Novagen, Darmstadt, Germany). Ubiquitin was amplified by PCR from an Ub-βGal plasmid with the primer 5′-GTTGAATTCAATGCAAATCTTCGTGAAGACTCTGACTGGTA-3′ and the antisense primer 5′-GTTAGATCTGAACCCACCTCTGAGACGGAGTACCA-3′ and inserted in frame in the EcoRI and BglII sites of the pACYCDuet-1 vector containing GFP. The underlined sequences represent restriction sites.

DUB assays. The GST-ORFs and Ub-GFP reporter plasmids were cotransfected by electroporation in competent BL21(DE3) bacteria that lack endogenous DUBs (9). Antibiotic-resistant colonies were selected in LB agar supplied with 100 μg of ampicillin/ml and 30 mg of chloramphenicol/ml. Exponentially growing bacteria (OD at 600 nm of 0.5) were induced for 5 h at 30°C with 0.5 mM IPTG (isopropyl-β-D-thiogalactopyranoside) and then lysed by sonication in phosphate-buffered saline supplemented with protease inhibitors (Complete Mini protease inhibitor cocktail tablets; Roche, Germany). The lysates were clarified by centrifugation for 10 min at 13,000 rpm, and cleavage of the reporter was analyzed by fractionation in acrylamide bis-Tris 4 to 12% precasted gradient gel (Invitrogen), followed by Western blotting. After transfer to polyvinylidene difluoride membrane (Millipore), the filter was blocked in phosphate-buffered saline supplemented with 5% nonfat milk and 0.1% Tween 20 and incubated for 1 h with anti-rabbit-GFP serum (Abcam, Cambridge, United Kingdom) diluted

1:10,000. After incubation for 1 h with peroxidase-conjugated goat anti-rabbit serum, the complexes were visualized by enhanced chemiluminescence (GE Healthcare, United Kingdom). For the enzyme kinetic assays, GST-USP19, GST-USP19mut, GST-BPLF1-N, GST-BSLF1, and GST-BXLF1 were purified from bacteria lysates (50 mM Tris-Cl [pH 7.5], 150 mM NaCl, 5 mM $MgCl_2$, 1% Triton X-100, 1 mM phenylmethylsulfonyl fluoride, 1 mM dithiothreitol) by incubation for 90 min at 4°C with a solution of 10 mM glutathione in 50 mM Tris-Cl (pH 8.0), and the protein concentrations were determined with a Bio-Rad protein assay. Hydrolysis of the fluorogenic substrate ubiquitin-AMC (Ub-AMC, SE211; Biomol) was assayed at 30°C in 100 μl of assay buffer (50 mM Tris-Cl [pH 7.5], 150 mM NaCl, 2 mM EDTA, 2 mM dithiothreitol) containing 200 nM concentrations of the enzyme, and the V_{max} and K_m of the reactions were calculated by titrating the substrate at concentrations ranging between 0 and 20 mM. The fluorescent product was measured by using a spectrofluorimetry plate reader at 380-nm excitation and 460-nm emission wavelengths. To block the DUB activity, 10 mM *N*-ethylmaleimide (NEM; Sigma) was added to the assay buffer.

Site-directed mutagenesis. Point mutations of the predicted catalytic Cys residues of BPLF1, BSLF1, and BXLF1 genes were engineered by using a QuikChange site-directed mutagenesis kit according to the manufacturer's protocol (Stratagene). Two BPLF1 mutants (C61A and C65A), three single mutants (C462A, C824A, and C819A), and one double mutant (C824/819A) of BSLF1 and two mutants of BXLF1 (C84A and C491A) were constructed. All constructs were then sequenced to verify that only the desired mutations had been introduced.

RESULTS

Four search strategies were used to identify putative DUBs encoded in the EBV genome: (i) sequence alignment with the conserved C- and H-boxes of known DUB families, (ii) pattern search of conserved catalytic domains, (iii) HMM-based searches, and (iv) identification of Cys and His residues that are conserved in homologues encoded by other members of the HHV family, followed by an HMM search.

Sequence alignment searches. A first attempt to identify putative DUBs was performed using CLUSTAL W to align the EBV ORFs with the human DUB data set. Three ORFs clustered with specific DUB subfamilies, BGLF4 and BBLF4 clustered with the OTU subfamily and BcLF1 ORF aligned with JAMMs (not shown), but the homologous regions did not contain Cys or His residues, and these viral ORFs are therefore unlikely to possess enzymatic activity. Since alignment of the entire amino acid sequence may not detect homology restricted to short domains that are critical for enzymatic activity, BLAST was used to identify EBV ORFs containing sequences of homology with the conserved C- and H-boxes of each DUB family using an arbitrary cutoff E-value of ≤10. Twenty-five candidates containing Cys or His residues in homologous regions were found in this search (see Table S1 in the supplemental material), including for example, the BBRF3 ORF that contains a region of strict homology with the USP C-box (E-value = 0.018).

Pattern search. Additional search strategies were conducted to achieve a more stringent assessment of the likelihood that the identified domains might be true C- or H-boxes homologues. Family-specific search patterns were derived from the aligned C- and H-box sequences of the known DUBs. To increase the stringency of the search, when fewer than 10 family members were found in the human data set, homologues from other species were also included in the alignment. The derivation of search patterns for the C- and H-boxes of the UCH family is illustrated in Fig. 1, and the search patterns for USP, OTU, MJD and JAMM families are given in Fig. S1A to D in the supplemental material. In a first attempt, stringent search patterns were derived for each DUB family (UCH, C-box −11/+11 and H-box −7/+16; USP, C-box −8/+7 and H-box −17/+3; OTU, C-box −8/+10 and H-box −8/+5; MJD, C-box −10/+10 and H-box −6/+7; and JAMM motif −7/+17) by including at each position all residues observed in the data set (Fig. 1B, boldface residues) and then used to search the EBV ORF data set, allowing for only a single mismatch. The derived patterns were in all cases able to identify the DUBs belonging to the family but failed to identify any candidate in the EBV ORFs (results not shown), suggesting that they may be too stringent to recognize distant homologues. Less-stringent search patterns were then derived by allowing at each position additional amino acids with similar physicochemical characteristics or, when residues with different physicochemical characteristics were observed, all amino acids (indicated by an "X" in Fig. 1B and in Fig. S1A to D in the supplemental material). Regions of similarity with the C- and/or H-boxes of different DUB families were identified in 30 EBV ORFs (see Table S2 in the supplemental material). Four ORFs contained at least one putative C-box and one H-box, while three ORFs contained only one putative C-box and twenty-three ORFs contained one or more H-box-like domain.

HMM search. Family-specific HMMs were derived for the aligned C- and H-boxes of the different DUB families. In order to increase the probability of identifying distant homologs, only sequences with <90% identity were included in the training set (Table 1). Since the EBV ORF database contains only 106 sequences and the HMMs are based on short C- and H-box domains of 13 to 24 aa, high E-values and low scores were expected. HMM alignments with E-values of ≤25 were therefore considered for further analysis. All hits containing Cys or His residues were further categorized based on the HMM scores (Table 2). Scores of ≥0, corresponding to more than 50% likelihood to be a true match, were considered high. Intermediate scores were between 0 and −6.6 (down to 1% probability to be a true match), while scores less than −6.6 were considered low. Seven EBV ORFs—BALF2, BALF5, BBRF3, BcLF1, BERF3-BERF4, BRLF1, and the predicted ORF88—contained at least one C- or H-box domain with score above 0, suggesting a potential homology with the corresponding DUB domains. Two ORFs—BNRF1 and BPLF1—contained both C- and H-box-like domains with scores ≥−6.6, and eighteen additional ORFs contained either a C- or an H-box-like domain with scores of less than −6.6.

Search for conserved Cys and His residues. A further attempt to identify candidate DUBs was undertaken based on the assumption that amino acid residues that are critical for protein function may be conserved in homologues encoded by different members of the HHV family. Homologous ORFs encoded by the known HHVs were identified by sequence comparison, and the conserved Cys and His residues were located. Twenty-one EBV ORFs contain at least one Cys or His residue that is conserved in homologues encoded by all HHV members, while Cys or His residues conserved only in α- or β-HHVs were detected in two and seven ORFs, respectively; thirteen EBV ORFs shared conserved Cys or His residues only with homologues encoded by the other member of the γ-HHV subfamily, KSHV, that resembles EBV in cell tropism and oncogenic capacity (see Table S3 in the supple-

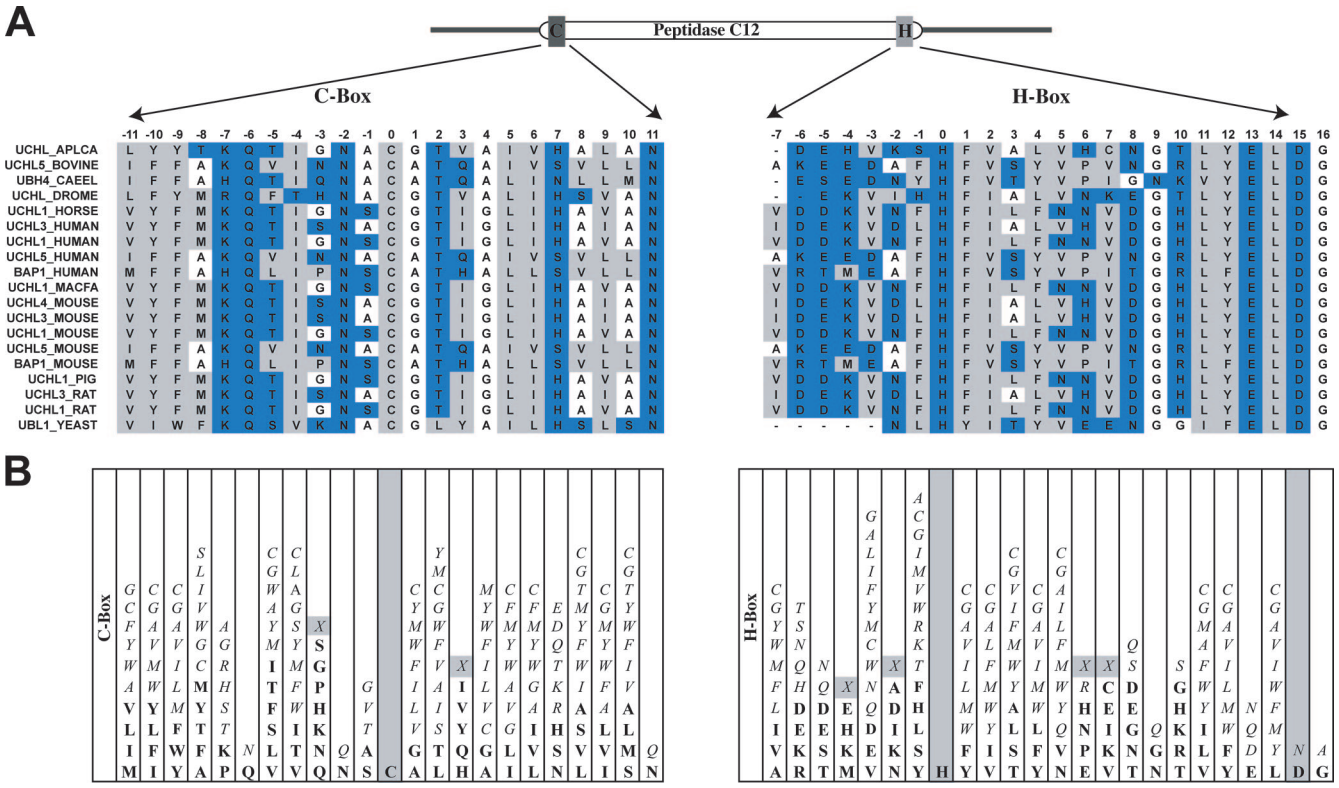

FIG. 1. Derivation of search patterns for the UCH subfamily catalytic domains. (A) The aligned amino acid sequences of the catalytic Cys and His-box regions of UCH (peptidase C12) family members are shown. The numbers above the alignment correspond to the amino acid position relative to the catalytic Cys and His residues. Polar residues are colored blue, hydrophobic residues are gray, and small residues (Gly and Ala) are white. (B) Stringent search patterns were derived by including at each position all amino acids observed in the aligned DUB sequences (indicated in bold). Less-stringent patterns were then obtained by allowing amino acids with similar physicochemical properties (indicated in italics). When different types of amino acids were observed at a given position, all amino acids were allowed in the pattern (indicated by X).

mental material). The sequences adjacent to the conserved residue were searched for putative C- and H-boxes using the DUB family specific HMMs. Nine EBV ORFs were found to contain conserved Cys or His residues located in regions homologous to the DUB C- or H-boxes, and one ORF, BGRF1/BDRF1, contained both C- and H-box homologous domains (see Table S3 in the supplemental material).

DUB score and exclusion criteria. A relatively large number of candidate DUBs were identified by at least one search, and several were identified by more than one. To select the most likely candidates for functional studies, scoring criteria were devised for each search, and these were then compiled in a global DUB score. The scores assigned to each search reflected the likelihood of identifying candidates that possess critical features associated with DUB activity (see Table S4 in the supplemental material). Candidates identified by the BLAST search were given a score of 1, 2, or 3 depending on the degree of similarity with DUB sequences. Candidates identified by the pattern search were scored 1 or 2 based on the presence of C- or H-box-like domains or both, while the score of candidates identified by the HMM considered both the presence of C- and H-box-like domain and their HMM scores (high = >0, intermediate = between 0 and −6.6, or low = <−6.6). The same scoring system was used for candidates identified by the presence of conserved Cys and His residues. The scores of 58 candidates identified by at least one search are shown in Table S4 in the supplemental material. Two ORFs—BGRF1/BDRF1 and BPLF1—were identified by the four searches, nine ORFs were identified by three searches, twenty-two ORFs were identified by two searches, and twenty-five ORFs were found by only one search. All candidates identified in at least three searches and five candidates identified by two searches received scores of ≥4. This group included 16 ORFs, all of which were identified by HMM, and 7 were shown to contain conserved Cys or His residues.

In order to further restrict the number of candidates to be validated by functional studies, ORFs with scores of ≥4 were scrutinized for the presence of structural constraints that could prevent DUB activity. The locations of the putative C- and H-boxes were mapped relative to each other and to other protein domains of known function (Fig. 2). Based on this domain analysis, the BBRF3 and BILF1 ORFs could be excluded since their putative C- and H-boxes are located in transmembrane regions, which would preclude DUB activity. Analysis of the site of expression in EBV-infected cells, expression during different phases of the virus cycle, and functional annotation (Table 3) revealed that some of the high-scoring candidates are structural proteins or glycoproteins associated with the virus capsid and envelope. These proteins are unlikely to possess enzymatic activity, although this cannot be excluded a priori. The remaining candidates include immediate-early, early, late, or latent proteins that are expressed in

TABLE 2. Putative DUB catalytic boxes identified by the HMM search[a]

EBV ORF	C-box		H-box	
	Type	Score	Type	Score
BALF1			OTU	*-0.4*
BALF2	OTU	**1.9**		
	UCH	*–6.4*		
BALF4	OTU	–10.2	UCH	–9.3
BALF5	USP	**0.3**		
BaRF1			UCH	*–1.9*
BBLF2	USP	*–2.9*		
BBLF4	MJD	–15	OTU	*–4.3*
BBRF2	USP	*–3.7*		
BBRF3	USP	**7.8**	OTU	–6.7
	UCH	–9.8		
BcLF1	OTU	**1.3**	OTU	*–4.2*
			USP	–8.4
BcRF1			MJD	–9.5
BDLF2			OTU	–7.6
BERF3-BERF4	USP	**0.69**		
	OTU	–7.9		
	MJD	–8.3		
BFRF2	OTU	–6.8		
BGLF1	OTU	*–1.6*	OTU	–7.7
BGLF2			OTU	*–4.6*
BGLF3			OTU	*–5.3*
BGRF1/BDRF1	MJD	–10.9	MJD	–8.1
BILF1	USP	*–0.6*		
BKRF1	USP	*–3*		
BLLF3			OTU	–7.9
BMLF1	OTU	–6.7		
BMRF2	MJD	–9.2		
BNRF1	USP	*–3.9*	OTU	*–2*
			UCH	–9.1
BORF1	USP	*–4.2*		
BPLF1	USP	*–4.5*	OTU	*–4.3*
BRLF1	USP	**0.9**	OTU	*–6.3*
	OTU	*–4.4*		
BSLF1	OTU	–7.8	OTU	–6.8
BVRF2	USP	*–3.5*	JAMM	–16.2
BXLF1	USP	*–3.4*	USP	–13.2
BXLF2			USP	*–5.2*
			UCH	*–5.5*
			MJD	–7.4
BXRF1			MJD	–8.9
LMP1	MJD	–8.4		
LMP2	USP	*–1*		
ORF101	USP	*–2.5*		
ORF35			OTU	*–5.3*
			MJD	–7.6
ORF42	OTU	–9.6		
ORF86	OTU	*–2.3*		
	USP	*–4.5*		
ORF88	OTU	–11.1	OTU	**2.9**

[a] The type of DUB domain found in each candidate is indicated as follows: USP, ubiquitin-specific protease; OTU, ovarian tumor domain protease; UCH, ubiquitin C-terminal hydrolase; MJD, Josephin domain protease. Boldfacing indicates high scores (>0); italics indicates intermediate scores (between 0 and −6.6); regular typeface indicates low scores (<–6.6)

the nucleus or, in one case, in the cytoplasm of the infected cells or are components of the viral tegument. It is noteworthy that two tegument proteins were found in the group with the highest DUB score and one of them, the protein encoded by the BPLF1 ORF, was previously shown to possess DUB activity (23, 42).

Functional validation of the candidates. In order to validate the DUB score, GST fusions of 11 EBV ORFs with scores of ≥4 and an approximately equal number of ORFs with scores of ≤3 were tested for their capacity to hydrolyze a Ub-GFP reporter plasmid coexpressed in bacteria. The results of a representative assay wherein the ORFs were tested alongside the human USP19 and a catalytic mutant that lacks enzymatic activity are shown in Fig. 3.

The reporter was efficiently cleaved by USP19, as confirmed by the detection of both free GFP (Fig. 3A) and free ubiquitin (data not shown), while cleavage was abolished by mutation of the catalytic Cys residue in the USP19Mut. In line with the reported DUB activity of this ORF, Ub-GFP was cleaved almost completely in bacteria expressing the N terminus of BPLF1 (Fig. 3A and B). The levels of cleavage significantly above background were also detected with BSLF1 and BXLF1, while the activity of BGRF1 and BALF5 was just below the cutoff (3 × the mean percent cleavage in the presence of ORFs with scores ≤3 [Fig. 3B]). The expression of the fusion proteins was in all cases confirmed in Western blots probed with anti-GST antibodies (data not shown). In order to further characterize their DUB activity, bacterially expressed GST-BPLF1-N, GST-BSLF1, and GST-BXLF1 were purified, and their enzyme activity was assayed by cleavage of the fluorogenic substrate Ub-AMC (Fig. 3C). The three EBV ORFs hydrolyzed Ub-AMC with different kinetics and K_m values, suggesting very different affinities for the substrate, but the specificity of the reaction was in all cases confirmed by blocking with the cysteine protease inhibitor NEM. Interestingly, the enzymatic activity of BSLF1 and BXLF1 relative to BPLF1 was significantly improved when equal amounts of immunoprecipitated proteins expressed in mammalian cells were compared for the cleavage of Ub-AMC (compare Fig. 3C and D), suggesting that posttranslational modifications that are not achieved in bacteria cells may be required for optimal activity.

In order to further validate the DUB activity of the candidates, the predicted catalytic Cys residues in BPLF1, BSLF1, and BXLF1 were mutated to Ala by using PCR-mediated site-directed mutagenesis, and the enzymatic activity of recombinant GST tagged proteins was tested against the Ub-AMC substrate (Fig. 4). Two putative C-boxes were predicted in the BSLF1 and BXLF1 ORFs, while a single domain containing two Cys residues was predicted in BPLF1. Alignment of the corresponding sequences in other members of the HHV family revealed that, while BPLF1 Cys61 and BSLF1 Cys819 and Cys824 are conserved in all HHVs, other potentially catalytic Cys residues identified by the bioinformatics search are unique for EBV or shared only by some of the family members. Mutation of the conserved C61 of BPLF1 to Ala abolished the enzymatic activity, while the C65A mutation had no effect, confirming that C61 is the catalytic residue in the C-box (Fig. 4). Single mutation of the nonconserved C462 and conserved C824 of BSLF1 did not affect the enzymatic activity, while the activity of the C819A mutant was significantly reduced. Interestingly, the hydrolysis of Ub-AMC was further decreased in the double mutant C819/824A, suggesting that C824 may partly substitute for the catalytic C819 residue. Homologs of BXLF1 were present only in alpha- and gammaherpesviruses, and the putative catalytic cysteine C491 is conserved only in gammaherpesvirus. Mutation of this residue abolished the enzymatic activity of BXLF1, while mutation of the nonconserved C84 had no effect (Fig. 4). Thus, catalytic Cys residues were iden-

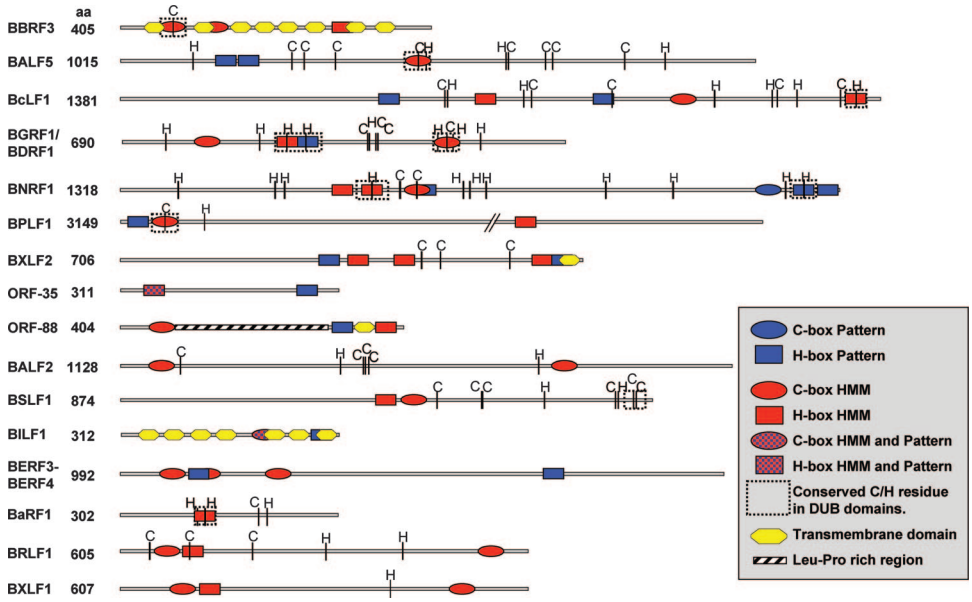

FIG. 2. Mapping of the putative C- and H-box domains in ORFs with high DUB scores. The positions of the putative C- and H boxes identified by the different searches and the Cys and His residues that are conserved in homologues encoded by other HHV family members are indicated. Putative transmembrane domains were identified by a TMHMM search in the candidate ORFs and are indicated as yellow hexagonal regions. In BBFR3, BILF1, and ORF88 the C- and/or B-boxes overlap with or flank transmembrane domains.

tified by mutation analysis in BPLF1, BSLF1, and BXLF1, confirming that the three EBV ORFs are bona fide viral DUBs.

To finally validate our bioinformatics approach, the scoring strategy used to identify BPLF1, BSLF1, and BXLF1 was applied to their homologues encoded by other human herpesviruses. All homologs of BPLF1 and BSLF1 received scores of ≥4, and several scored even higher than the EBV-encoded protein (Table 4). This is in line with the reported DUB activity of several BPLF1 homologues. In agreement with the very low sequence similarity of the BXLF1 homologues expressed in alpha- and gammaherpesvirus these ORFs received very low DUB scores, suggesting that this protein may have different functions in different viruses.

DISCUSSION

In this study we used a bioinformatics approach to identify distant functional homologues of human ubiquitin deconjugases encoded in the EBV genome. This task is complicated by the great genetic variability of viruses, which results in poor sequence conservation even between homologous proteins expressed by different members of the same virus family. Indeed, currently used bioinformatics tools, such as BLAST searches

TABLE 3. ORF annotation and filtering criteria

EBV ORF	DUB score[a]	EBV protein	Homologue			Expression in virus cycle	Location	Function[b]	Filter
			HSV	CMV	KSHV				
BBRF3	9	Glycoprotein M	gM	gM	gM	Late	Envelope	M	(–)
BcLF1	7	Major capsid protein	UL19	UL86	ORF25	Late	Capsid	C	–
BALF5	7	DNA pol catalytic subunit	UL30	UL54	ORF9	Early	Nucleus	R	
BGRF1/BDRF1	7	DNA packaging, Terminase	UL15	UL89	ORF29	Late	Nucleus	P	
BNRF1	6	Major tegument protein			ORF75	Late	Tegument	T	
BPLF1	6	Large tegument protein	UL36	UL48	ORF64	Late	Tegument	T	
BXLF2	5	gp85, gH homologue	UL22	UL75	ORF22	Late	Envelope	M	(–)
ORF35	5	Hypothetical							
ORF88	5	Hypothetical							–
BALF2	5	ssDNA binding protein	UL29	UL57	ORF6	Early	Nucleus	R	
BSLF1	5	Helicase/primase complex	UL52	UL70	ORF56	Early	Nucleus	R	
BILF1	4	gp64, constitutive GPCR				Early	Membrane	M	(–)
BERF3-BERF4	4	EBNA3C				Latent	Nucleus	L	
BaRF1	4	RNase reductase	UL40		ORF60	Early	Nucleus	N	
BRLF1	4	Rta, transactivator			ORF50	I-Early	Nucleus	S	
BXLF1	4	Thymidine kinase	UL23		ORF21	Early	Nucleus	N	

[a] For the details on the scoring, see Table S4 in the supplemental material.
[b] Classification of protein based on function: C, capsid; M, membrane protein; N, nucleotide metabolism; L, latency; P, packaging; R, replication; S, signaling, transactivator, transcription factor; T, tegument.

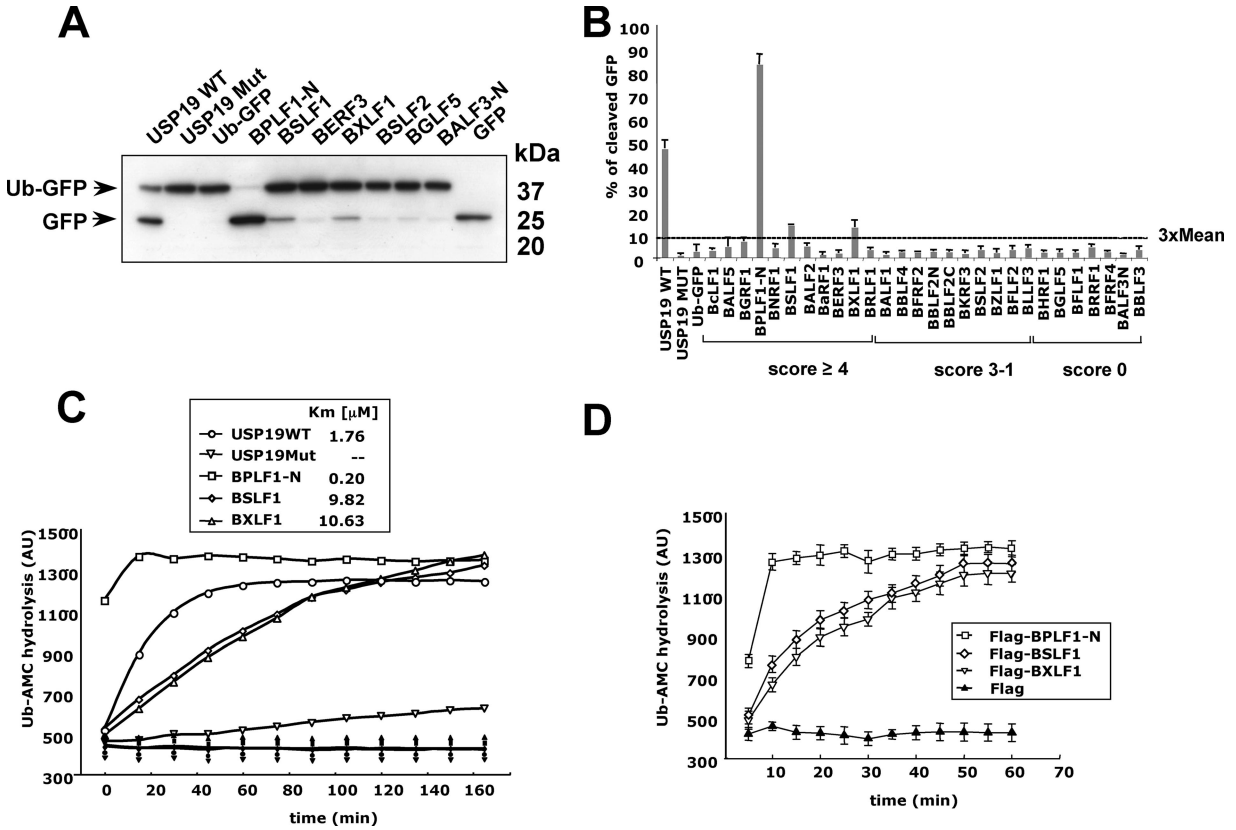

FIG. 3. Functional validation of the candidate DUBs. (A) Representative Western blot illustrating cleavage of the Ub-GFP reporter by a restricted panel of EBV ORFs. BL21 cells were cotransfected with Ub-GFP, and the indicated ORF and protein expression was induced by treatment with IPTG. Cell lysates were fractionated on 4 to 12% sodium dodecyl sulfate-polyacrylamide gel electrophoresis gradient gels, and GFP was detected by Western blotting. Cleavage of the reporter in lysates expressing active DUBs is visualized by appearance of a free GFP band. (B) Enzymatic activity of candidate EBV DUBs (score ≥ 4) and controls (score ≤ 3). The intensity of the bands corresponding to the uncleaved reporter and free GFP was determined by densitometry, and the percent specific cleavage was calculated as follows: intensity of the free GFP band – background/total GFP (uncleaved + cleaved) – background $\times$ 100. A cutoff activity value was calculated as 3 $\times$ the mean percent specific cleavage in cells expressing ORFs with a score of ≤ 3. The mean of three experiments in which all of the ORFs were tested in parallel is shown in the figure. (C) Time course of Ub-AMC hydrolysis. Ub-AMC (1.2 μM) was mixed with 200 nM concentrations of purified GST-USP19wt, GST-USP19mut, GST-BPLF1-N, GST-BSLF1, and GST-BXLF1 in the absence (empty symbols) or presence (filled symbols) of NEM, and the reactions were monitored for 180 min. The release of fluorescent AMC, expressed in arbitrary units (AU), shows the activity of these enzymes to cleave Ub-AMC. The K_m of the reactions was calculated in separate experiments and is indicated in the Figure. (D) Time course of Ub-AMC hydrolysis of BPLF1, BSLF1, and BXLF1 expressed in mammalian cells. The ORFs were cloned in frame in the 3XFlag tag vector and expressed in HEK293 cells. The proteins were immunoprecipitated from the transfected cells using antibodies to the Flag tag, and the cleavage of Ub-AMC was assayed as described for panel C. Equal amounts of proteins were used in all enzymatic assays. The faster kinetics of Ub-AMC cleavage (compare panels C and D) indicates that the enzymatic activity of mammalian expressed BSLF1 and BXLF1 is significantly improved compared to the proteins expressed in bacteria.

or more sophisticated threading programs that use sequence alignment and protein fold recognition algorithms, fail to detect homologies between known viral and cellular DUBs, suggesting that the structural properties of the viral proteases are clearly distinct. This was recently confirmed by the crystal structure of a DUB encoded by the murine gammaherpesvirus M48 that, based on the arrangement of the active-site residues and the architecture of the ubiquitin interacting interface, was classified as the first member of a new class of DUBs (43).

We reasoned that, in spite of strongly divergent sequences, a higher degree of conservation might be expected in regions that are important for enzymatic activity. Thus, although the homology between the catalytically relevant regions of viral and cellular enzymes falls below the statistically significant cutoffs used in conventional searches, distant homologues may be identified using less-stringent search criteria. The human genome encodes for approximately 95 DUBs subdivided in five families (38). Although the sequences of individual DUBs vary widely, the members of each family share a high degree of homology in regions surrounding conserved Cys and His residues that form the catalytic core of the enzymes. We therefore focused on the identification of EBV ORFs containing a region of homology with the C- and H-boxes of each DUB family and scored the candidates based on the degree of homology with the consensus sequences and on the presence of only one or both types of consensus domains. Four different strategies based on sequence alignment, pattern search, HMM motifs, and detection of conserved Cys and His residues in the context of HMM motifs were used to search for putative C- and H-boxes. The use of multiple searches provides a distinct advan-

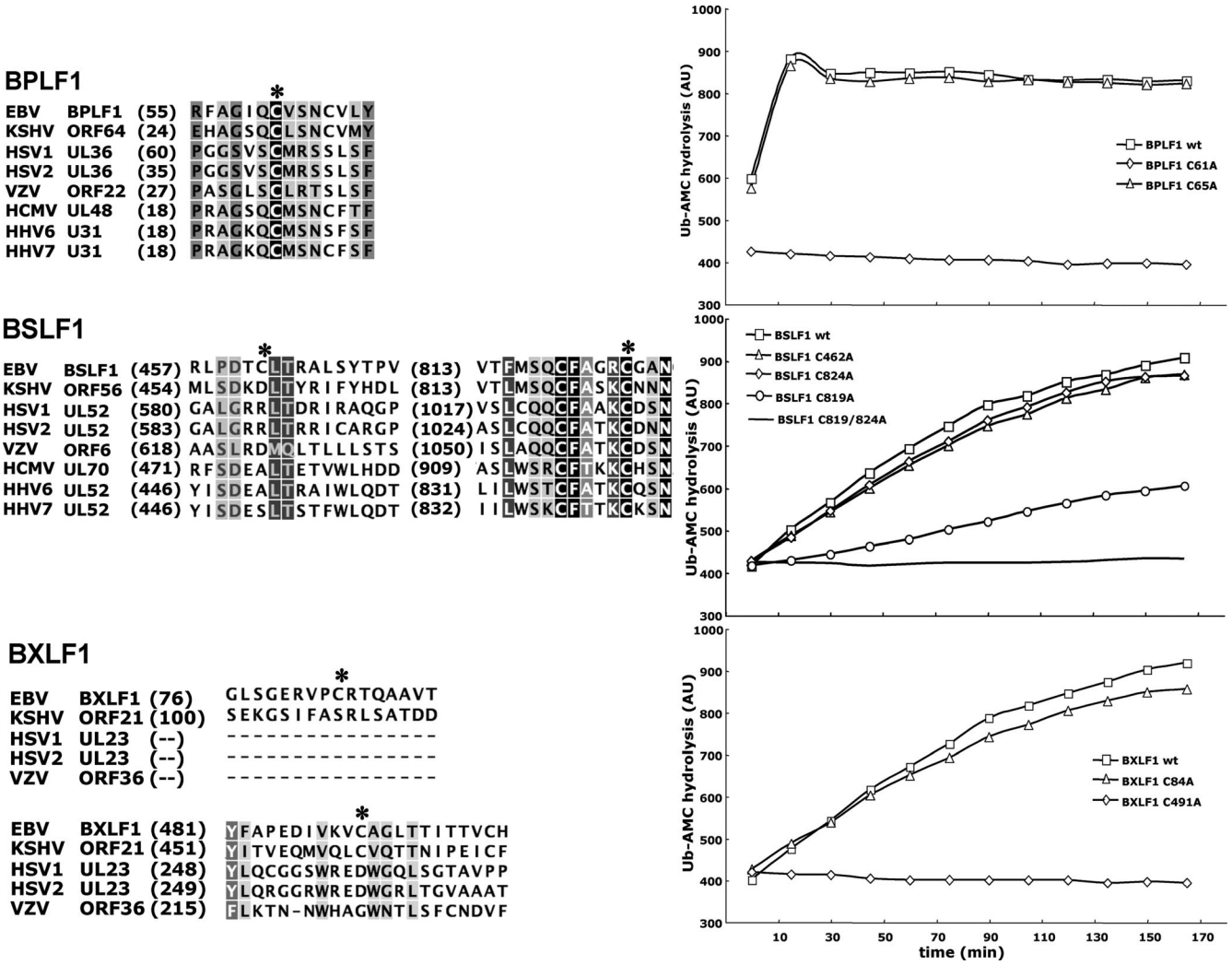

FIG. 4. Identification of the catalytic Cys residues by site-directed mutagenesis. Sequence alignments of the putative catalytic C-boxes in BPLF1, BSLF1, and BXLF1 and their homologs encoded by other HHV members shows conservation of Cys residues that are involved in DUB activity. The conserved residues are shown in white text with a black background, while similar residues in the alignment are shaded in gray. The asterisk above the alignment indicates the Cys residues identified in the bioinformatics search. Mutations were introduced into the predicted catalytic Cys residues, and the ability of the mutants to hydrolyze Ub-AMC was assayed as described in the legend to Fig. 3.

tage since each search is biased by different criteria. Thus, while sequence alignment scores for the presence of a continuous sequence of homologous residues, the pattern search restricts the hits to sequences that share similar residues at critical positions in the motif and HMM gives a global score based on the likelihood that a given residue will be found in each position of the motif. A further refinement of the HMM search was based on the assumption that functionally relevant proteins will be conserved among members of a virus family, and therefore conserved Cys and His residues will be found in the putative catalytic domains. By assigning individual scores to each of these searches and then combining the scores into a global DUB score, we have identified 16 candidates with DUB scores of $\geq$4 out of 106 annotated or predicted ORF in the EBV genome. Five of the candidates were excluded from further analysis because the putative catalytic domains are located within or at the opposite sides for transmembrane domains or because they are either known structural components of the virus capsid or envelope glycoproteins and are therefore unlikely to possess DUB activity.

A previously identified viral DUB encoded by the BPLF1 ORF was found among the high score candidates. BPLF1 is the EBV homologue of UL36, a presumably multifunctional protein of the alphaherpesvirus HSV-1. DUB activity was previously mapped to the N-terminal portion of UL36 by using a functional proteomic approach based on labeling of total cell extracts with and epitope-tagged, Ub-based suicide substrates followed by immunoprecipitation, and identification of the labeled enzyme by mass spectrometry (23). Using a reporter substrate that carries ubiquitin fused to GFP in a conformation that mimics the ubiquitin precursors and, to some extent, a true ubiquitinated substrate, we have now confirmed that the N terminus of BPLF1 is a very potent ubiquitin deconjugase. Interestingly, two additional ORFs in the high-score group, BSLF1 and BXLF1, were also capable of cleaving Ub-GFP at levels significantly above background. The enzymatic activity of

TABLE 4. DUB scores for the herpesvirus homologs of the identified EBV DUBs

ORF	Virus	Search score				Global DUB score[a]
		BLAST	Pattern	HMM	Conserved	
		1	1	2	2	6
ORF64	KSHV	1	1	2	2	6
UL36	HSV-1	2	1	2	2	7
UL36	HSV-2			2	2	4
ORF22	VZV		1	2	2	5
UL48	CMV	3	2	3	3	11
U31	HHV-6	2	1	2	2	7
U31	HHV-7		1	2	2	5
BSLF1	EBV	2		2	1	5
ORF56	KSHV	2	1	1	1	5
UL52	HSV-1	1	1	2	2	6
UL52	HSV-2	1		2	1	4
ORF6	VZV		1	2	2	5
UL70	CMV	2	1	2	2	7
UL52	HHV-6	3		2	1	6
UL52	HHV-7	2	1	2	1	6
BXLF1	EBV	2		2		4
ORF21	KSHV		1			1
UL23	HSV-1					-
UL23	HSV-2		1			1
ORF36	VZV				1	1

[a] For the details on the scoring, see Table S4 in the supplemental material.

the new putative DUBs was in both cases confirmed by the capacity of the purified GST fusion proteins to cleave the fluorogenic substrate Ub-AMC. Furthermore, the catalytic Cys residues were identified in both proteins by mutation analysis, confirming that these EBV ORFs are bona fide DUBs. It is noteworthy that bacterially expressed full-length BSLF1 and BXLF1 exhibited a poor enzymatic activity compared to both the N-terminal portion of BPLF1 and the human DUB USP19 that was included as control. Comparison of the enzymatic activity of purified proteins expressed in mammalian cells suggests that this may be due to the requirement for posttranslational modifications that are not achieved in bacteria. Indeed, only the N terminus of UL36 was identified in the functional screen performed in HSV-1-infected cells, suggesting that the protein may be processed during infection.

The new viral DUBs identified in the present study are expressed in the nucleus of EBV-infected cells during the early phases of the productive virus cycle and, based on their annotated functions, are involved in DNA replication and nucleotide metabolism. It is noteworthy that the efficiency and fidelity of DNA replication is regulated by posttranslational modification of several components of the replication complex, including for example, monoubiquitination, polyubiquitination, and sumoylation of PCNA (36). The BSLF1 gene product shares 23% sequence identity with HSV UL52, the primase component of the trimolecular helicase-primase complex was shown to be essential to HSV replication (12, 13). In EBV the complex is made up of BSLF1, BBLF4 (UL5 homolog), and BBLF2/3 (UL8 homolog) (51), but its activity in viral replication has not been directly confirmed. Similar to UL52, BSLF1 contain several conserved amino acid domains, such as the DxD motif (aa 481 to 498) and a putative zinc finger (Znf; aa 782 to 829) motif at the C-terminal end of protein that are also found in prokaryotic and eukaryotic primases (7, 15, 24). Mutational analysis of the Znf of HSV UL52 showed that this region is required for the virus replication (7, 8, 10). The Znf of BSLF1 partially overlaps with the predicted catalytic C-box.

BXLF1 gene encodes a protein of 607 aa that was annotated as the EBV thymidine kinase (TK) gene due to its capacity to complement TK-negative strains of *E. coli* (30) and partial sequence homology with regions of HSV-1 TK (19). We found that the regions that identify BXLF1 as a putative DUB and the catalytic Cys residue are not conserved in other herpesvirus homologues. Moreover, in contrast to other family members, BXLF1 was shown to localize to the centrosomes, where it encircles the tubulin-rich centrioles in a microtubule-independent manner (20). It remains to be seen whether this atypical localization may reflect a dual enzymatic activity that is not present in the homologues.

In conclusion, we have shown that it is possible to use bioinformatics tools to identify distant homologues of DUBs encoded by viruses. Our strategy of choosing candidates based on a global DUB score obtained by combining the results of multiple low stringency searches identified 16 high scoring ORFs in a database of 106 putative or confirmed EBV ORFs. Enzymatic activity was confirmed for 3 of 11 ORFs tested, whereas ORFs with low score and ORFs lacking putative C- or H-boxes were uniformly negative. Thanks to its relatively good predictive capacity, our approach could provide a valuable complement to the functional screening described by Kattenhorn et al. (23), which, due to the requirement for validation by mass spectroscopy, is strongly biased toward enzymes that are overexpressed in the infected cells. Further studies will be required to assess how the DUB activity of BPLF1, BSLF1, and BXL1 contributes to their role in virus replication and to the remodeling of the cellular environment during productive EBV infection.

ACKNOWLEDGMENTS

We thank Joel Hedlund for help with the sequence clustering procedure.

This study was supported by grants from the Swedish Cancer Society, the Swedish Medical Research Council, and the Karolinska Institutet, Stockholm, Sweden (to M.G.M. and K.L.); by the Carl Trygger Foundation and Linköping University (to B.P.); by Bayerisches Genomeforschungsnetzwork and MRC G0501453 (to J.H.); and by the European Community Integrated Project on Infection and Cancer, project LSHC-CT-2005-018704 (to M.G.M.).

REFERENCES

1. **Altschul, S. F., W. Gish, W. Miller, E. W. Myers, and D. J. Lipman.** 1990. Basic local alignment search tool. J. Mol. Biol. **215:**403–410.
2. **Amerik, A. Y., and M. Hochstrasser.** 2004. Mechanism and function of deubiquitinating enzymes. Biochim. Biophys. Acta **1695:**189–207.
3. **Baer, R., A. T. Bankier, M. D. Biggin, P. L. Deininger, P. J. Farrell, T. J. Gibson, G. Hatfull, G. S. Hudson, S. C. Satchwell, C. Seguin, et al.** 1984. DNA sequence and expression of the B95-8 Epstein-Barr virus genome. Nature **310:**207–211.
4. **Bairoch, A., R. Apweiler, C. H. Wu, W. C. Barker, B. Boeckmann, S. Ferro, E. Gasteiger, H. Huang, R. Lopez, M. Magrane, M. J. Martin, D. A. Natale, C. O'Donovan, N. Redaschi, and L. S. Yeh.** 2005. The universal protein resource (UniProt). Nucleic Acids Res. **33:**D154–D159.
5. **Balakirev, M. Y., M. Jaquinod, A. L. Haas, and J. Chroboczek.** 2002. Deubiquitinating function of adenovirus proteinase. J. Virol. **76:**6323–6331.
6. **Barretto, N., D. Jukneliene, K. Ratia, Z. Chen, A. D. Mesecar, and S. C. Baker.** 2005. The papain-like protease of severe acute respiratory syndrome coronavirus has deubiquitinating activity. J. Virol. **79:**15189–15198.
7. **Biswas, N., and S. K. Weller.** 1999. A mutation in the C-terminal putative Zn^{2+} finger motif of UL52 severely affects the biochemical activities of the HSV-1 helicase-primase subcomplex. J. Biol. Chem. **274:**8068–8076.

8. **Carrington-Lawrence, S. D., and S. K. Weller.** 2003. Recruitment of polymerase to herpes simplex virus type 1 replication foci in cells expressing mutant primase (UL52) proteins. J. Virol. **77:**4237–4247.
9. **Catic, A., S. Misaghi, G. A. Korbel, and H. L. Ploegh.** 2007. ElaD, a deubiquitinating protease expressed by *Escherichia coli*. PLoS ONE **2:**e381.
10. **Chen, Y., S. D. Carrington-Lawrence, P. Bai, and S. K. Weller.** 2005. Mutations in the putative zinc-binding motif of UL52 demonstrate a complex interdependence between the UL5 and UL52 subunits of the human herpes simplex virus type 1 helicase/primase complex. J. Virol. **79:**9088–9096.
11. **Ciechanover, A., A. Orian, and A. L. Schwartz.** 2000. Ubiquitin-mediated proteolysis: biological regulation via destruction. Bioessays **22:**442–451.
12. **Crute, J. J., and I. R. Lehman.** 1991. Herpes simplex virus-1 helicase-primase: physical and catalytic properties. J. Biol. Chem. **266:**4484–4488.
13. **Crute, J. J., T. Tsurumi, L. A. Zhu, S. K. Weller, P. D. Olivo, M. D. Challberg, E. S. Mocarski, and I. R. Lehman.** 1989. Herpes simplex virus 1 helicase-primase: a complex of three herpes-encoded gene products. Proc. Natl. Acad. Sci. USA **86:**2186–2189.
14. **D'Andrea, A., and D. Pellman.** 1998. Deubiquitinating enzymes: a new class of biological regulators. Crit. Rev. Biochem. Mol. Biol. **33:**337–352.
15. **Dracheva, S., E. V. Koonin, and J. J. Crute.** 1995. Identification of the primase active site of the herpes simplex virus type 1 helicase-primase. J. Biol. Chem. **270:**14148–14153.
16. **Drake, J. W.** 2006. Chaos and order in spontaneous mutation. Genetics **173:**1–8.
17. **Eddy, S. R.** 1998. Profile hidden Markov models. Bioinformatics **14:**755–763.
18. **Frias-Staheli, N., N. V. Giannakopoulos, M. Kikkert, S. L. Taylor, A. Bridgen, J. Paragas, J. A. Richt, R. R. Rowland, C. S. Schmaljohn, D. J. Lenschow, E. J. Snijder, A. Garcia-Sastre, and H. W. ten Virgin.** 2007. Ovarian tumor domain-containing viral proteases evade ubiquitin- and ISG15-dependent innate immune responses. Cell Host Microbe **2:**404–416.
19. **Gardberg, A., L. Shuvalova, C. Monnerjahn, M. Konrad, and A. Lavie.** 2003. Structural basis for the dual thymidine and thymidylate kinase activity of herpes thymidine kinases. Structure **11:**1265–1277.
20. **Gill, M. B., J. L. Kutok, and J. D. Fingeroth.** 2007. Epstein-Barr virus thymidine kinase is a centrosomal resident precisely localized to the periphery of centrioles. J. Virol. **81:**6523–6535.
21. **Hershko, A., and A. Ciechanover.** 1998. The ubiquitin system. Annu. Rev. Biochem. **67:**425–479.
22. **Hewitt, E. W., L. Duncan, D. Mufti, J. Baker, P. G. Stevenson, and P. J. Lehner.** 2002. Ubiquitylation of MHC class I by the K3 viral protein signals internalization and TSG101-dependent degradation. EMBO J. **21:**2418–2429.
23. **Kattenhorn, L. M., G. A. Korbel, B. M. Kessler, E. Spooner, and H. L. Ploegh.** 2005. A deubiquitinating enzyme encoded by HSV-1 belongs to a family of cysteine proteases that is conserved across the family *Herpesviridae*. Mol. Cell **19:**547–557.
24. **Klinedinst, D. K., and M. D. Challberg.** 1994. Helicase-primase complex of herpes simplex virus type 1: a mutation in the UL52 subunit abolishes primase activity. J. Virol. **68:**3693–3701.
25. **Kovalenko, A., C. Chable-Bessia, G. Cantarella, A. Israel, D. Wallach, and G. Courtois.** 2003. The tumour suppressor CYLD negatively regulates NF-κB signalling by deubiquitination. Nature **424:**801–805.
26. **Larsen, C. N., J. S. Price, and K. D. Wilkinson.** 1996. Substrate binding and catalysis by ubiquitin C-terminal hydrolases: identification of two active site residues. Biochemistry **35:**6735–6744.
27. **Lee, J. C., and M. E. Peter.** 2003. Regulation of apoptosis by ubiquitination. Immunol. Rev. **193:**39–47.
28. **Lehner, P. J., S. Hoer, R. Dodd, and L. M. Duncan.** 2005. Downregulation of cell surface receptors by the K3 family of viral and cellular ubiquitin E3 ligases. Immunol. Rev. **207:**112–125.
29. **Lindner, H. A., N. Fotouhi-Ardakani, V. Lytvyn, P. Lachance, T. Sulea, and R. Menard.** 2005. The papain-like protease from the severe acute respiratory syndrome coronavirus is a deubiquitinating enzyme. J. Virol. **79:**15199–15208.
30. **Littler, E., J. Zeuthen, A. A. McBride, E. Trost Sorensen, K. L. Powell, J. E. Walsh-Arrand, and J. R. Arrand.** 1986. Identification of an Epstein-Barr virus-coded thymidine kinase. EMBO J. **5:**1959–1966.
31. **Loureiro, J., and H. L. Ploegh.** 2006. Antigen presentation and the ubiquitin-proteasome system in host-pathogen interactions. Adv. Immunol. **92:**225–305.
32. **Lu, G., and E. N. Moriyama.** 2004. Vector NTI, a balanced all-in-one sequence analysis suite. Brief Bioinform. **5:**378–388.
33. **Lynch, O. T., and M. Gadina.** 2004. Ubiquitination for activation: new directions in the NF-κB roadmap. Mol. Interv. **4:**144–146.
34. **Masucci, M. G.** 2004. Epstein-Barr virus oncogenesis and the ubiquitin-proteasome system. Oncogene **23:**2107–2115.
35. **Menard, R., H. E. Khouri, C. Plouffe, R. Dupras, D. Ripoll, T. Vernet, D. C. Tessier, F. Laliberte, D. Y. Thomas, and A. C. Storer.** 1990. A protein engineering study of the role of aspartate 158 in the catalytic mechanism of papain. Biochemistry **29:**6706–6713.
36. **Moldovan, G. L., B. Pfander, and S. Jentsch.** 2007. PCNA, the maestro of the replication fork. Cell **129:**665–679.
37. **Nijman, S. M., T. T. Huang, A. M. Dirac, T. R. Brummelkamp, R. M. Kerkhoven, A. D. D'Andrea, and R. Bernards.** 2005. The deubiquitinating enzyme USP1 regulates the Fanconi anemia pathway. Mol. Cell **17:**331–339.
38. **Nijman, S. M., M. P. Luna-Vargas, A. Velds, T. R. Brummelkamp, A. M. Dirac, T. K. Sixma, and R. Bernards.** 2005. A genomic and functional inventory of deubiquitinating enzymes. Cell **123:**773–786.
39. **Rice, P., I. Longden, and A. Bleasby.** 2000. EMBOSS: the European molecular biology open software suite. Trends Genet. **16:**276–277.
40. **Rytkonen, A., J. Poh, J. Garmendia, C. Boyle, A. Thompson, M. Liu, P. Freemont, J. C. Hinton, and D. W. Holden.** 2007. SseL, a *Salmonella* deubiquitinase required for macrophage killing and virulence. Proc. Natl. Acad. Sci. USA **104:**3502–3507.
41. **Scheffner, M., B. A. Werness, J. M. Huibregtse, A. J. Levine, and P. M. Howley.** 1990. The E6 oncoprotein encoded by human papillomavirus types 16 and 18 promotes the degradation of p53. Cell **63:**1129–1136.
42. **Schlieker, C., G. A. Korbel, L. M. Kattenhorn, and H. L. Ploegh.** 2005. A deubiquitinating activity is conserved in the large tegument protein of the herpesviridae. J. Virol. **79:**15582–15585.
43. **Schlieker, C., W. A. Weihofen, E. Frijns, L. M. Kattenhorn, R. Gaudet, and H. L. Ploegh.** 2007. Structure of a herpesvirus-encoded cysteine protease reveals a unique class of deubiquitinating enzymes. Mol. Cell **25:**677–687.
44. **Schwartz, A. L., and A. Ciechanover.** 1999. The ubiquitin-proteasome pathway and pathogenesis of human diseases. Annu. Rev. Med. **50:**57–74.
45. **Shackelford, J., and J. S. Pagano.** 2004. Tumor viruses and cell signaling pathways: deubiquitination versus ubiquitination. Mol. Cell. Biol. **24:**5089–5093.
46. **Sun, L., and Z. J. Chen.** 2004. The novel functions of ubiquitination in signaling. Curr. Opin. Cell Biol. **16:**119–126.
47. **Thompson, J. D., D. G. Higgins, and T. J. Gibson.** 1994. CLUSTAL W: improving the sensitivity of progressive multiple sequence alignment through sequence weighting, position-specific gap penalties and weight matrix choice. Nucleic Acids Res. **22:**4673–4680.
48. **Uetz, P., Y. A. Dong, C. Zeretzke, C. Atzler, A. Baiker, B. Berger, S. V. Rajagopala, M. Roupelieva, D. Rose, E. Fossum, and J. Haas.** 2006. Herpesviral protein networks and their interaction with the human proteome. Science **311:**239–242.
49. **Verma, R., L. Aravind, R. Oania, W. H. McDonald, J. R. Yates III, E. V. Koonin, and R. J. Deshaies.** 2002. Role of Rpn11 metalloprotease in deubiquitination and degradation by the 26S proteasome. Science **298:**611–615.
50. **Wing, S. S.** 2003. Deubiquitinating enzymes: the importance of driving in reverse along the ubiquitin-proteasome pathway. Int. J. Biochem. Cell. Biol. **35:**590–605.
51. **Yokoyama, N., K. Fujii, M. Hirata, K. Tamai, T. Kiyono, K. Kuzushima, Y. Nishiyama, M. Fujita, and T. Tsurumi.** 1999. Assembly of the Epstein-Barr virus BBLF4, BSLF1 and BBLF2/3 proteins and their interactive properties. J. Gen. Virol. **80**(Pt. 11)**:**2879–2887.
52. **Zhou, H., D. M. Monack, N. Kayagaki, I. Wertz, J. Yin, B. Wolf, and V. M. Dixit.** 2005. *Yersinia* virulence factor YopJ acts as a deubiquitinase to inhibit NF-κB activation. J. Exp. Med. **202:**1327–1332.